

Optimize Distillation Columns

Distillation is the dominant process for separating large multi-component streams into high purity products. So, the chemical process industries' ongoing quest to improve energy utilization, reduce capital costs, and boost operating flexibility is spurring increasing attention to distillation column optimization during design. Designers often approach column optimization in an iterative manner, heavily relying on vendor experience and information. A good understanding of mass-transfer and pressure-drop fundamentals, as they relate to optimization, will enable the column designer to independently judge vendor offerings and effectively determine the optimal equipment design.

This article will address the following optimization goals: (1) maximizing theoretical stages per height of section or column, (2) minimizing pressure drop per theoretical stage, and (3) maximizing the operational range, turn-down, or turn-up.

Application of mass-transfer and pressure-drop fundamentals can lead to improved designs for both trayed and packed columns.

A distillation column can use either trays or packings. Their mechanisms of mass transfer differ, but the key for both is a good approach to equilibrium through the generation of large amounts of interfacial area. This interfacial area results from the passage of vapor through the perforations of trays, or the spreading of liquid on the surface of packings.

First, we will discuss the underlying phenomena for trayed columns and the design approaches that can be used to meet the three optimization goals. Then, we will address the mechanisms and approaches for packed columns. Finally, we will consider the selection of trays vs. packing.

Part I: Trayed columns

DOUGLAS L. BENNETT
AND KENNETH W. KOVAK,
AIR PRODUCTS AND CHEMICALS, INC.

In a trayed column, liquid flows down the column through downcomers and then across the tray deck, while vapor flows upward through the liquid inventory on the tray. Tray designs can be divided into cross-flow and parallel-flow types. Figure 1 illustrates the conceptual differences. Cross-flow trays are the most common and least expensive, but parallel-flow trays, if properly designed, can provide an efficiency that is 10% or more higher. Figure 1 depicts a single-pass cross-flow tray. By “pass,” we mean the number of downcomers per tray. As column diameter increases, the ratio

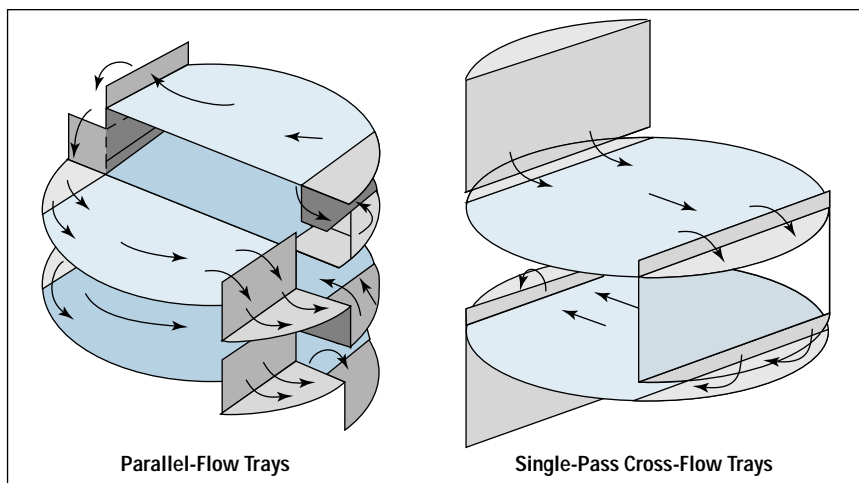


Figure 1. Types of trays.

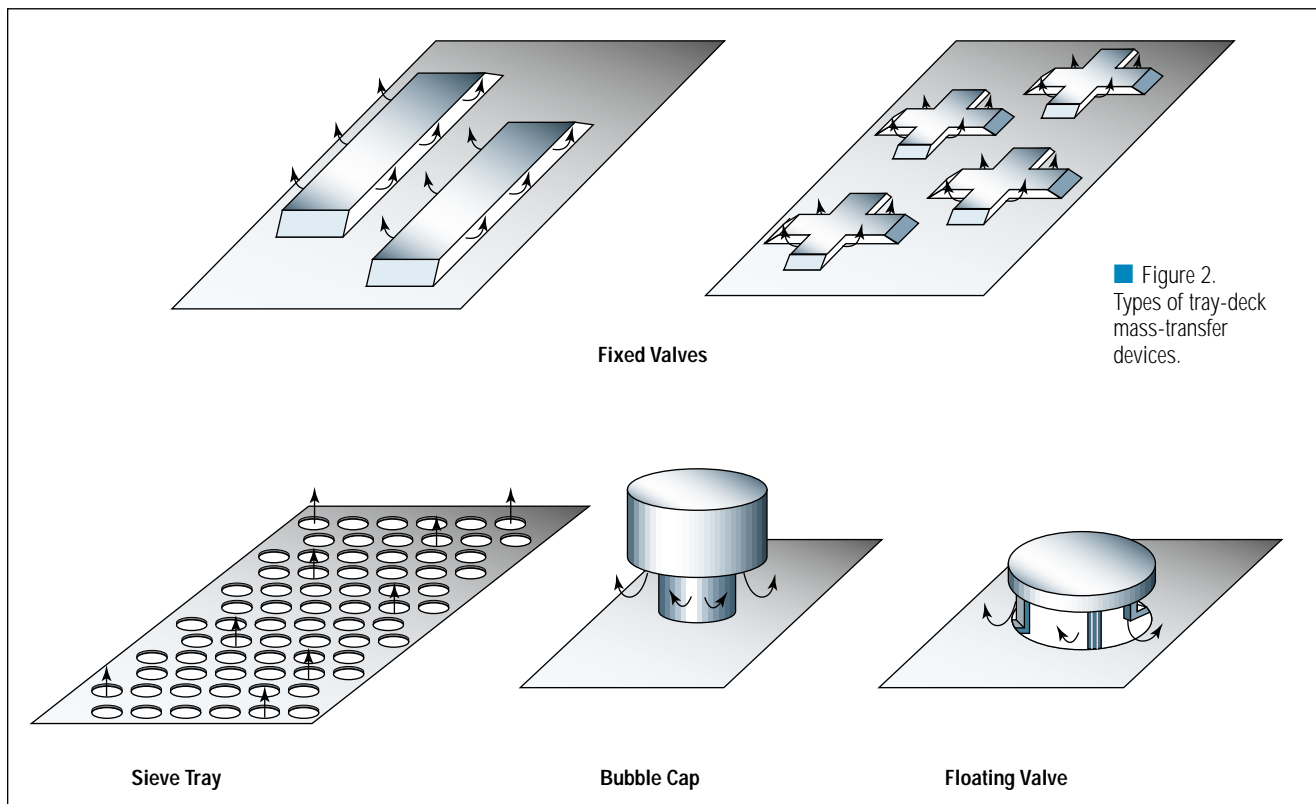


Figure 2.
Types of tray-deck
mass-transfer
devices.

Nomenclature

A_B	= area of perforated portion of tray deck
A_H	= total hole area
D	= molecular diffusivity
D_H	= sieve-tray perforation diameter
Fr_L	= liquid Froude number = $[\rho_v V_H^2 / \rho_L g h_L]^{0.5}$
E	= ratio of liquid entrainment mass flow to upward column vapor mass flow
h_D	= tray pressure-drop component associated with vapor flowing through perforation, expressed in height of clear liquid
h_{Fe}	= effective froth height as defined by Bennett <i>et al.</i> (2)
h_L	= liquid inventory on tray, expressed in height of clear liquid
h_T	= total tray pressure drop expressed in height of liquid
h_O	= tray pressure-drop component associated with formation of bubbles expressed in height of liquid
$h_{2\phi}$	= height of two-phase region on the tray, see Figure 4
g	= acceleration due to gravity
K_S	= density-corrected superficial gas velocity over bubbling surface = $[\rho_v / (\rho_L - \rho_v)]^{0.5} V_S$
L	= liquid mass-flow rate through column
m	= slope of equilibrium curve
T_S	= tray spacing
V	= vapor mass-flow rate through column
V_H	= velocity of the vapor through perforation hole
V_S	= velocity of vapor over bubbling surface of the tray

Greek letters

β	= constant defined in Bennett <i>et al.</i> (1) = $0.5 [1 + \tanh(1.3 \ln(h_T/D_H) - 0.15)]$
ρ	= density
μ	= viscosity
η_{PT}	= point efficiency
η_{SECT}	= tray section efficiency, ratio of number of theoretical stages to number of trays in a section
ϕ_e	= effective froth density, h_L/h_{Fe} , as defined in Bennett <i>et al.</i> (2)
$\phi_{2\phi}$	= $h_L/h_{2\phi}$

Subscripts

L	= liquid
ML	= liquid molar
MV	= vapor molar
V	= vapor
Opt	= optimum

of weir length to throughput decreases; so, for larger dia. columns, multi-pass trays often are used to increase weir length and achieve about the same liquid inventory on the tray.

The performance of a tray also depends upon the type of tray deck. The simplest is a sieve tray — it has a perforated tray deck with a uniform hole diameter of from less than a millimeter to about 25 mm. Trays with valves, which can be fixed or floating, also are very common; bubble caps still are used, but infrequently and usually only for extreme turndown. Figure 2 shows representatives of each family.

Tray efficiency depends upon column throughput. As seen in Figure 3, there is a relatively flat, stable operation region characterized by a gradual increase in efficiency as vapor hole velocity and liquid inventory rise with throughput. On either side of this stable region, performance drops off. The drop-off at low rates results first from weeping and then more significantly from dumping. At high rates, heavy entrainment decreases efficiency and then performance dramatically drops when flooding occurs. Because our optimization goals often will require operation at the extremes of the stable region, it is helpful to understand the controlling mechanisms in these three regions.

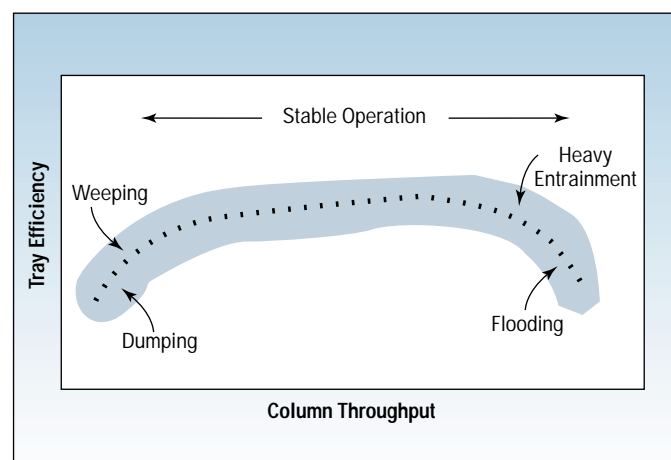


Figure 3. Tray performance vs. throughput.

Weeping and dumping

Weeping and dumping are related but different phenomena. During weeping, a minor fraction of liquid flows to the tray below through the tray perforations rather than the downcomer. This downward-flowing liquid typically has been exposed to rising vapor; so, weeping only leads to a small reduction in overall tray efficiency, to a level rarely worse than the tray point efficiency. In contrast, during dumping, a substantial portion of liquid flowing down the column passes through a region of the perforated tray deck. Often, most of this liquid has not been exposed to the rising vapor; therefore, performance degrades significantly — frequently resulting in overall tray efficiency being significantly less than local point efficiency.

Weeping and dumping differ in their underlying mechanisms. For large-perforation sieve trays, vapor and liquid can flow in an approximately steady, countercurrent manner through a perforation. More likely, however, especially for sieve trays with smaller perforations, weeping is transient, resulting in spurts of liquid leaving a nonbubbling perforation. The spurting occurs when there is a local and instantaneous downward pressure imbalance over the perforation. The cause of this imbalance can be associated with the bubbling frequency or, because the flow on a

large-scale tray is very complex, the imbalance can stem from local density and height variations of the froth waves traveling on the tray. The result is weeping regions that tend to move around on the tray deck. Dumping is much more extreme and occurs because, at the intended tray throughput, there is insufficient vapor pressure drop to retain entering liquid on the tray deck. Thus, significant quantities of liquid flow through a portion of the tray that has little if any vapor flow. Flow over the outlet weir can be zero. Normally minor phenomena, for example, the hydraulic gradient or tray-inlet liquid flow maldistribution, can have a significant impact on the minimum tray pressure drop required to prevent dumping and where on the tray the dumping occurs — and, therefore, on the level of performance degradation.

Stable operation

It is easiest to discuss this region by considering the simplest tray deck design, a perforated plate. In this case, vapor flows upward through the perforations and enters a two-phase layer of height $h_{2\phi}$. Vapor momentum is at its maximum as the vapor accelerates through the perforation. The exchange of this vapor momentum with the liquid inventory on the tray deck is critical to the nature of the two-phase zone. The two-phase layer can be spray-like or froth-like. Bennett *et al.* (1) have shown that the ratio of the liquid inventory, h_L , to the perforation diameter, D_H , is key to this momentum exchange. When h_L/D_H exceeds about 2, vapor momentum is exchanged with significant quantities of liquid; the two-phase mixture is largely liquid-continuous and behaves as a froth with reasonable mass transfer. When h_L/D_H is under about 1, vapor momentum is exchanged with little liquid; the two-phase region is largely vapor-continuous with significant upward liquid and vapor velocity components. The resulting flow regime is spray-like with poor mass transfer.

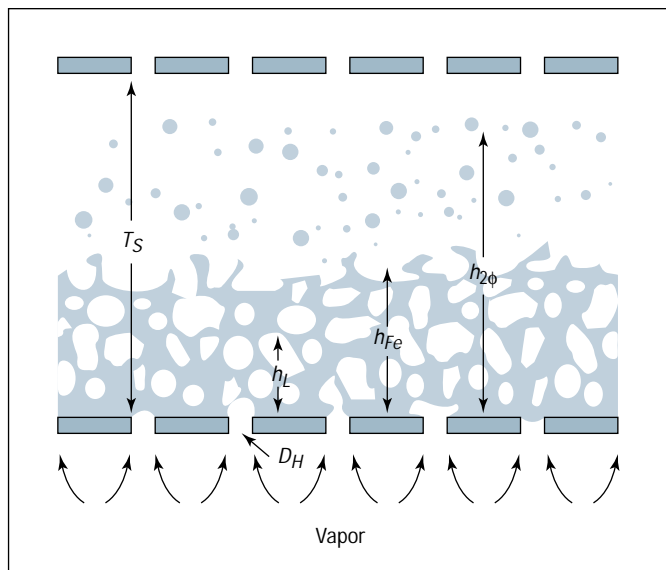


Figure 4. Froth flow structure.

Spray-like flows should be avoided if at all possible — if they cannot be avoided in a tray design, a packed column often is a better choice.

Because spray-like conditions should be avoided, we will concentrate in this article on froth flow. Figure 4 illustrates some of the main parameters of interest. The tray deck is spaced a distance of T_s from adjacent trays. The bulk of liquid is contained within a liquid-continuous region near the tray deck that has a height about equal to the effective froth height, h_{Fe} , as defined by Bennett *et al.* (2). A smaller portion of liquid inventory is contained as droplets in the vapor-continuous region above the liquid-continuous region. The velocity of these liquid droplets is related to the vapor momentum through the perforation and the ratio h_L/D_H ; if the vertical component of velocity is sufficient, droplets will be carried to the tray above.

Most of the liquid inventory and interfacial area occur within the liquid-continuous region; therefore, this part of the total two-phase region is most important for both pressure drop and mass transfer. Smaller perforation sizes, by increasing h_L/D_H , promote the exchange of momentum of the vapor to the liquid and, thus, the deceler-

ation of vapor velocity within the liquid-continuous layer. The resulting lower average vapor velocity within this layer increases vapor residence time; lower values of D_H and higher values of h_L enhance mass-transfer efficiency within the stable operation region.

Heavy entrainment and flooding

At high throughputs, corresponding to the top of the stable operation region, significant quantities of liquid droplets reach the tray deck above and pass through to the upper tray. This recirculation, called entrainment, degrades the composition profile in the column. If the downcomer can handle this additional liquid traffic, the column can tolerate significant entrainment and operate in a stable manner, but with a lower number of theoretical stages. At high values of entrainment, the column control system may no longer allow stable operation and the column behavior can enter a condition that is best called “operational” flood. (Some have called this jet flood, but this term is misleading because jetting often is used as a synonym for the spray-like regime and an operational flood can occur for either spray-like

$$\eta_{PT} = 1 - \exp \left[\frac{-0.0029}{1 + m \frac{\rho_{MV}}{\rho_{ML}} \sqrt{\frac{D_V(1-\phi_e)}{D_L \left(\frac{A_H}{A_B}\right)}}} \left(\frac{\rho_V V_H h_{Fe}}{\mu_V} \right)^{0.4136} \left(\frac{h_L}{D_H} \right)^{0.6074} \left(\frac{A_H}{A_B} \right)^{-0.3195} \right] \quad (1)$$

or froth-like conditions.) The occurrence of operational flood depends upon the control system and the sensitivity of the overall tray efficiency to entrainment (for example, parameters λ , L/V , and η_{PT}). Not all columns and control systems will lead to an operational flood at high entrainment.

There is a critical distinction between operational flood and hydraulic flood. Hydraulic flood results when the downcomer, at a given column throughput, becomes fully loaded with liquid and entrained vapor, and this mixture within the downcomer begins to impede flow over the outlet weir. The added resistance increases tray liquid inventory and pressure drop. This, in turn, raises the two-phase mixture height in the downcomer area, further impeding flow over the outlet weir, and boosting pressure drop even more. Finally, at hydraulic flood, all the liquid that enters the column no longer can leave the column; liquid is accumulated above the flood point and pressure drop increases rapidly. In contrast, in operational flood, all the liquid entering the column section still leaves the column, even though pressure drop can be very high and efficiency is very poor or unstable.

Some mass-transfer and pressure-drop fundamentals

We will use the recent correlation for sieve-tray efficiency reported by Bennett *et al.* (3). They address point efficiency, entrainment, mixing within the froth, weeping, and cross-flow and parallel-flow tray types. Their correlation for point efficiency is given in Eq. 1 above. This equation underscores many of the trends that we will quantify with further analysis. It

uses a Reynolds number, $\rho_V V_H h_{Fe} / \mu_V$, that other studies have shown to have an impact on bubble size. Larger values of the vapor velocity through the perforation, V_H , yield higher interfacial area. As expected, the ratio h_L/D_H plays a significant role. The ratio of hole area to bubbling surface area, A_H/A_B , also is important: smaller values enhance efficiency. The denominator of the first term within the major brackets is the correction required when liquid-phase resistance is important.

When the objective is to minimize the pressure drop per theoretical stage, pressure drop also must be calculated; we will use the method of Bennett *et al.* (2) for these calculations:

$$h_T = h_L + h_D + h_\sigma \quad (2)$$

where h_T is tray pressure drop, h_L is liquid inventory, h_D is pressure drop of the vapor flowing through the perforation, and h_σ is pressure drop associated with bubble formation.

Bennett *et al.* (3) report that, for their composite database for cross-flow trays, weeping did not appear to substantially degrade performance as long as the Froude number:

$$Fr_L = \left(\frac{\rho_V V_H^2}{\rho_L g h_L} \right)^{0.5} \geq 0.5 \quad (3)$$

At high vapor rates, entrainment becomes significant and decreases tray performance. To take this into account, we will use the correlation for entrainment given by Bennett *et al.* (3):

$$E = 0.00335 \left(\frac{T_s}{h_{2\phi}} \right)^{-1.10} \left(\frac{\rho_L}{\rho_V} \right)^{0.5} \phi_{2\phi}^\beta \quad (4)$$

where $h_{2\phi}$ is given by Eq. 5 below.

We will account for the degradation in tray efficiency caused by entrainment, but also will assume that hydraulic flood or operational flood will not be encountered.

The approach used

There are no generalized correlations that apply to all types of tray-deck designs. So, our approach will be to use the broadly based correlations developed for sieve trays to develop some optimization rules and then to discuss the implications of using other types of trays on these rules. The optimization goals are: (1) maximizing theoretical stages per section or column height, (2) minimizing pressure drop per theoretical stage, and (3) maximizing the operational range, turn-down, or turn-up.

We chose single-variable perturbations, assuming a constant liquid-to-vapor mass flow ratio, L/V , for each example. To test our answers, we selected properties consistent with a number of model systems: methanol and water (170 and 310 kPa), low-pressure C_6/C_7 (27 and 165 kPa), and high-pressure *iso/normal* butane (2,000 and 2,800 kPa). With these systems, the vapor density, ρ_V , varied from 1 to about 100 kg/m³, the liquid density, ρ_L , from 370 to 750 kg/m³, and $\rho_V/(\rho_L - \rho_V)$ from 0.015 to 0.36. We also looked at a full range of typical tray-geometry parameters,

$$h_{2\phi} = h_{Fe} + 7.79 \left[1 + 6.9 \left(\frac{h_L}{D_H} \right)^{-1.85} \right] \frac{K_s^2}{\phi_e g \left(\frac{A_H}{A_B} \right)} \quad (5)$$

values of L/V , and vapor throughputs corresponding to a density-corrected superficial gas velocity, K_S , from 0.025 to 0.06 m/s. In this manner, we were able to quantify the general impact of changing individual geometry parameters. More details are contained in Bennett *et al.* (4).

The optimization results

The ratio of section efficiency to pressure drop, η_{SECT}/h_T , is the number of stages per unit liquid height of pressure drop, higher values being more energy efficient. In Figure 5a, typical values of this ratio are plotted vs. the perforation diameter. Smaller values of D_H enhance efficiency through promotion of froth over spray, and through better mass transfer resulting from smaller bubbles. At very small values of D_H , tray pressure drop rises substantially due to bubble-formation pressure drop. In Figure 5b, we see a similar plot indicating that a relatively gentle optimum occurs at large values of open area. As the percent open area goes up, pressure drop declines at a faster rate than efficiency, thereby giving an increase in η_{SECT}/h_T . As the fraction open area continues to rise past this point, mass transfer drops as the Reynolds number decreases. This plot ignores weeping. Further analysis shows, however, that this optimum generally occurs when weeping is expected to begin, which for cross-flow trays is at approximately $Fr_L = 0.5$. This gives:

$$\left. \frac{A_H}{A_B} \right|_{Opt} = \left. \frac{A_H}{A_B} \right|_{Fr_L=0.5} = 2 K_S \sqrt{\frac{1}{g h_L}} \tag{6}$$

When maximizing η_{SECT}/h_T , there also is an optimal weir height. This optimum can exist because, at larger values of outlet weir, pressure drop increases at a higher rate than efficiency. At very low values of outlet weir height, liquid inventory is less, which cuts tray efficiency, but tray pressure drop decreases less rapidly, because h_D be-

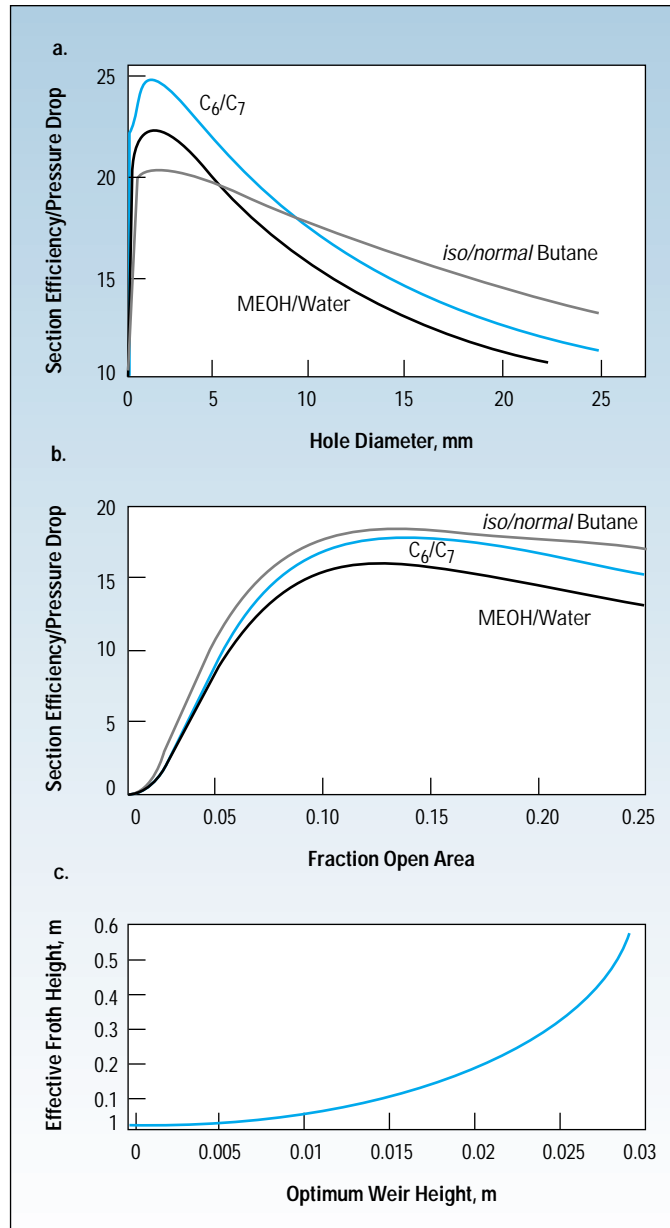


Figure 5. Distillation energy efficiency.

gins to dominate. Figure 5c gives a plot of calculated optimum weir height vs. effective froth density, where effective froth height is given by:

$$h_{Fe} = \frac{h_L}{e^{-12.55 (K_S)^{0.91}}} \quad \text{with } K_S \text{ in m/s} \tag{7}$$

The parameter η_{SECT}/T_S is the number of theoretical stages per height of column. Higher values

mean that more stages can be achieved within a given column height. In Figure 6a, typical values for this parameter are plotted vs. fraction open area. As fraction open area decreases, vapor velocity through the perforation increases, giving more interfacial area. At extremely small values of open area, vapor velocity through the perforations is very large — this promotes entrainment and thus degrades overall tray efficiency. In Figure

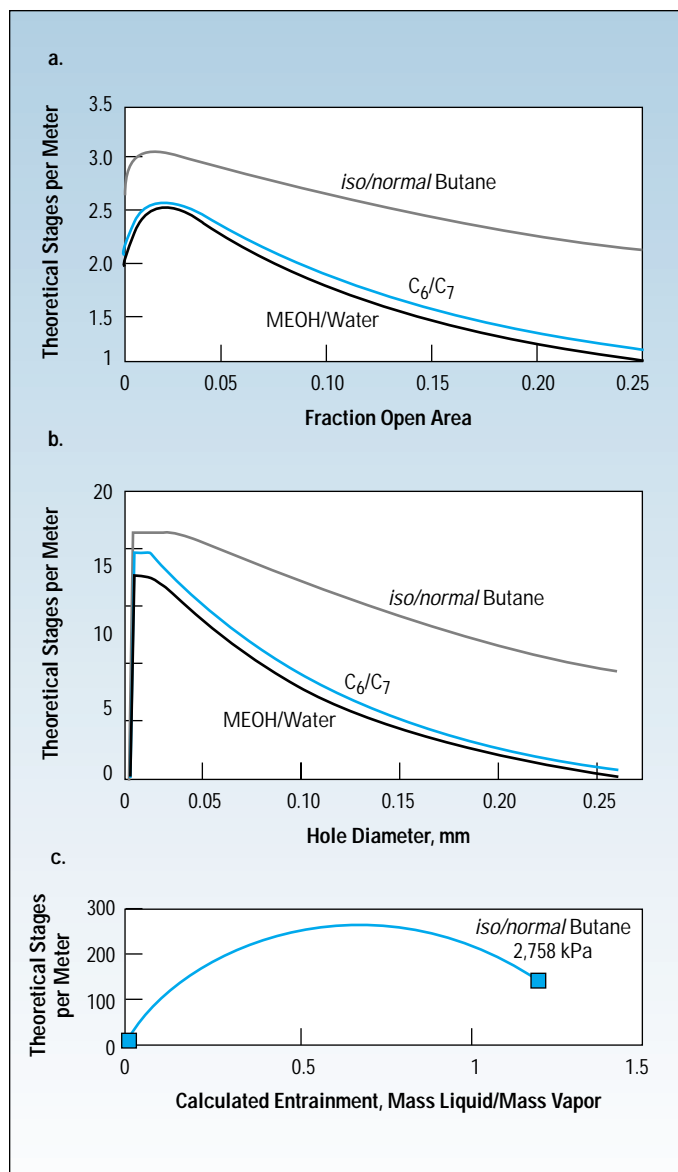


Figure 6. Maximizing the number of stages per column height.

mass-of-entrained-liquid-to-mass-of-vapor-throughput ratio of 0.1 to 0.2, is advantageous. Of course, the downcomer must be appropriately designed to accommodate this.

Summary of rules

To maximize the number of theoretical stages for a given section height:

For sieve trays:

1. Keep the fraction open area low, for example, in the range of 5%.

2. Use the smallest practical perforation diameter. This value will depend upon the degree of system fouling, the ability to clean fouled trays, and the tray deck material and thickness.

3. If practical, select a tray spacing that yields high entrainment — a tray spacing corresponding to an entrained-liquid-to-vapor-flow ratio of about 0.2 is reasonable, if confidence in the entrainment rate exists and downcomer capacity is adequate.

4. Consider parallel flow trays, if the cost increase is justified. Bennett *et al.* (3) show that opting for such trays generally leads to an enhancement of 10% or more in the number of theoretical stages.

For other types of trays:

Trays with small fixed valves can be used with success. Such designs have a relatively large open area, but a smaller perforation size compared to larger fixed or floating valves. In addition, the vapor must flow around the impact region of the valve and this decreases upward momentum and entrainment. Selecting a tray spacing that results in a reasonable level of entrainment also is effective. Parallel-flow valve trays would lead to more theoretical trays within a given column height, but valve designs that do not disturb the liquid flow pattern on the tray should be selected. Trays using very small bubble caps also could be advantageous, because the vapor is forced to initially flow downwards to the tray floor and this can enhance efficiency.

6b, η_{SECT}/T_S is plotted vs. perforation hole diameter. Small perforations give better mass-transfer efficiency. The minimum hole size for a tray, however, depends upon structural considerations and the fouling characteristics of the distillation system.

It is intuitively obvious that, if the rise in liquid entrainment is reasonable, installing more trays will increase the theoretical stages per column height. Figure 6c illustrates calculated values for η_{SECT}/T_S vs. calculated entrainment rate. These calcula-

tions assume that effective froth heights are less than tray spacing (and ignore questions about the impact of entrained liquid on tray hydraulics). This assumption is not valid at the very small tray spacing implied by the high entrainment values given in Figure 6c, but these results do show that significant amounts of liquid entrainment can occur prior to reaching a maximum value of η_{SECT}/T_S . If tray efficiency per column height is important, operating trays with a significant amount of entrainment, for example, at a

Sieve trays normally have a better efficiency than cap trays; so, unless extreme turndown is particularly important, the added cost of small bubble-cap trays is not justified.

To minimize the pressure drop per theoretical stage:

For sieve trays:

1. Use the largest fraction open area that will not result in weeping. Based on the literature for cross-flow trays, this maximum occurs around:

$$\left. \frac{A_H}{A_B} \right|_{Fr_L=0.5} = 2 K_s \sqrt{\frac{1}{g h_L}} \quad (8)$$

The open literature does not address this for parallel-flow trays.

2. Use the smallest practical perforation diameter.

3. Specify a low outlet weir, generally less than 50 mm.

4. Consider parallel-flow trays, if the cost increase is justified.

For other types of trays:

The pressure drops of trays with fixed valves and bubble caps often can be larger than those for sieve trays, if the sieve trays are designed at maximum values of the fraction of open area. The increase in hydraulic resistance for valve and bubble-cap trays also boosts tray pressure drop and can lead to dumping of liquid through the valves or caps, frequently at the tray entrance. Techniques have been developed to mitigate this effect, but more pressure drop usually results. Tray deck features with smaller openings will promote smaller bubbles and better efficiency. Lower outlet weirs and parallel-flow trays can offer efficiency advantages.

To maximize the operating range:

For sieve trays:

1. Reducing the fraction open area decreases the onset of weeping and increases entrainment. In general, however, our study has shown that lower open areas will maximize the operating range.

2. Decreasing the tray perforation diameter to the minimum practical size will decrease entrainment and will not adversely impact weeping.

3. Maximizing the tray spacing will raise maximum throughput and not adversely impact weeping, but also will lower the number of stages within a given column height.

4. Decreasing the liquid inventory by increasing the number of tray passes or lowering the weir height will enhance turn-down and generally will cut entrainment for a given column throughput. Reducing the outlet weir height below 25 mm, however, offers little advantage. The lower liquid inventory also will decrease tray efficiency. The spray-like regime must be avoided.

5. Some high-capacity tray designs with downcomers that allow liquid to drop onto the tray deck below can result in weeping through the tray openings under the downcomer. For such designs, the turn-down capability of the tray can be reduced by an unacceptable amount of bypass to the tray below.

For other types of trays:

Sieve trays, when properly designed to maximize operating range, can have an operating range of good and stable performance of about a factor of two or more, if larger tray spacing and higher pressure drop at peak rates are acceptable. Floating

valves, because their minimum flow area varies with vapor throughput, can have a wider operating range — about a factor of three — with a lower maximum pressure drop than sieve trays, but often with a lower efficiency and a higher cost. Small-size fixed-valves generally will have a greater maximum range than large-size fixed or floating valves when tray count per section height is also important and a larger pressure drop at maximum rates is acceptable. Their ability to turn down, however, is not as great as floating valves. Small-size bubble caps, although expensive, can have substantial turn-down capability and, with special design considerations to prevent liquid/vapor bypass at extreme turn-down, can give an operating range greater than a factor of five. CEP

D. L. BENNETT is General Manager, Advanced Gas Separation, for Air Products and Chemicals, Inc., Allentown, PA ((610) 481-7788; Fax: (610) 706-7420; E-mail: bennetdl@apci.com). He has worked for the company for 24 years, during which time he has held a number of senior-level technical and management positions. He has authored over 60 publications, many in the separations area. He has been granted 12 patents, and has several others pending. He received a BA in applied science as well as BS, MS, and PhD degrees in mechanical engineering, all from Lehigh Univ. A member of AIChE, he is a Director of the Institute's Separations Div. He also serves on the Board of Directors of Fractionation Research, Inc. In 1992, he received the Chairman's Award, the highest and most-prestigious award given by Air Products, for his contributions to cryogenic technology.

K. W. KOVAK is Technology Manager, Cryogenic Systems — Air Separation, for Air Products and Chemicals, Inc., Allentown, PA ((610) 481-6464; Fax: (610) 481-2177; E-mail: kovakkw@apci.com). In his 22 years at the company, he has held various process engineering, management, and technology positions. He has over 20 years of experience in the design, manufacture, and operation of cryogenic processing systems, particularly for cryogenic distillation. He received BS and MS degrees in chemical engineering from Manhattan College. He is a member of AIChE and of the Institute's Separations Div.

Literature Cited

1. **Bennett, D. L., A. S. Kao, and L. W. Wong**, "A Mechanistic Analysis of Sieve Tray Froth Height and Entrainment," *AIChE J.*, **41** (9), p. 2,067 (Sept. 1995).
2. **Bennett, D. L., R. Agrawal, and P. J. Cook**, "New Pressure Drop Correlation for Sieve Tray Distillation Columns," *AIChE J.*, **29** (3), p. 434 (May 1983).
3. **Bennett, D. L., D. Watson, and M. A. Wiscinski**, "New Correlation for Sieve-Tray Point Efficiency, Entrainment, and Section Efficiency," *AIChE J.*, **43** (6), p. 1,611 (June 1997).
4. **Bennett, D. L., K. W. Kovak, and D. Zak**, "Optimization of Sieve-Type Distillation Trays," presented at AIChE Annual Meeting, Los Angeles (1997).

Part II: Packed columns

DOUGLAS L. BENNETT,
AIR PRODUCTS AND CHEMICALS, INC.

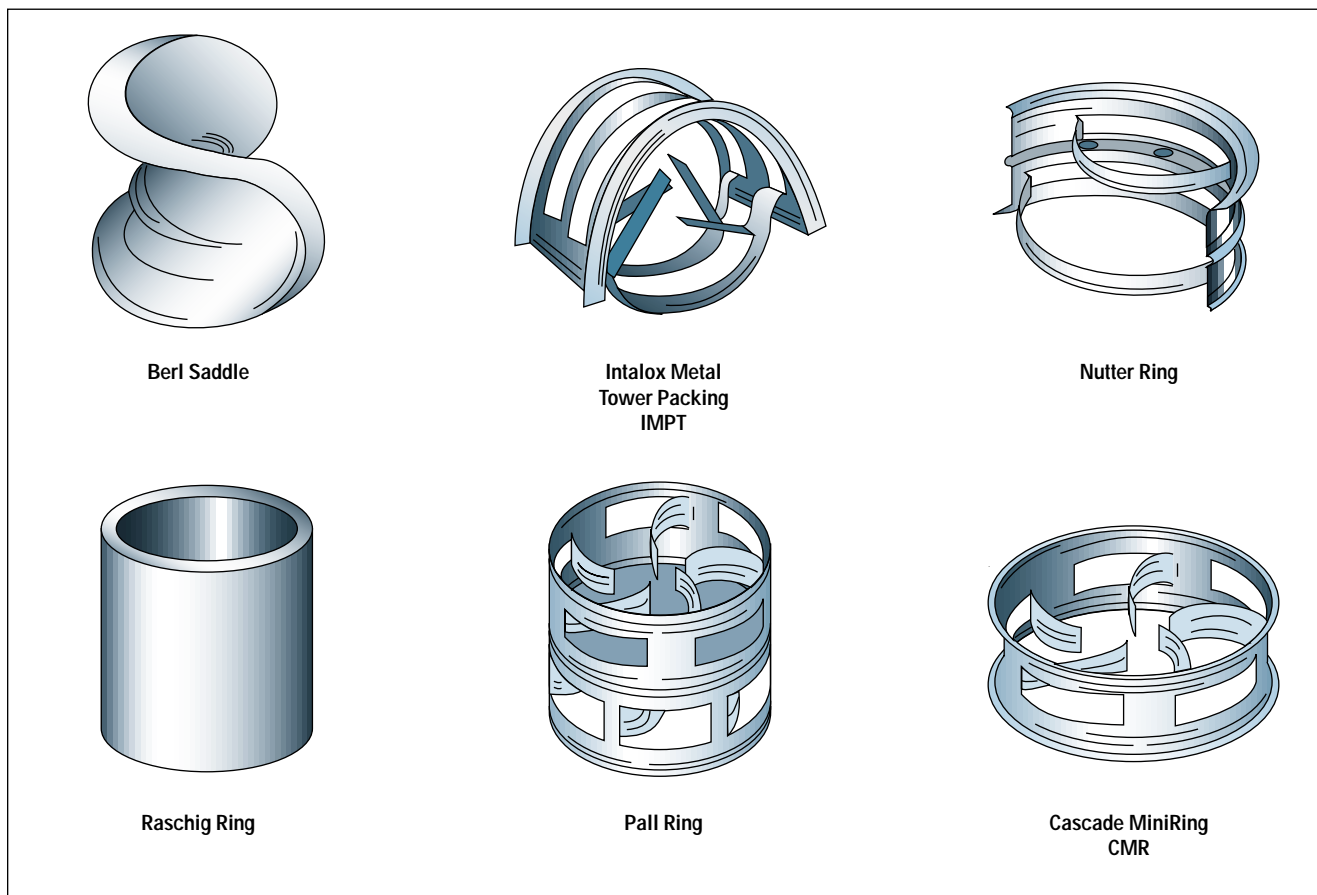
The wide range of commercial packings and their variations in geometry introduce significant empiricism into the design of packed columns. Application of fundamental mass-transfer and pressure-drop principles, however, still can lead to the identification of general optimization rules. As we did for trayed columns, here we will develop rules for the following optimization goals: (1) maximizing theoretical stages per height

of section or column, (2) minimizing pressure drop per theoretical stage of separation, and (3) maximizing the operating range of the column that results in reasonable performance.

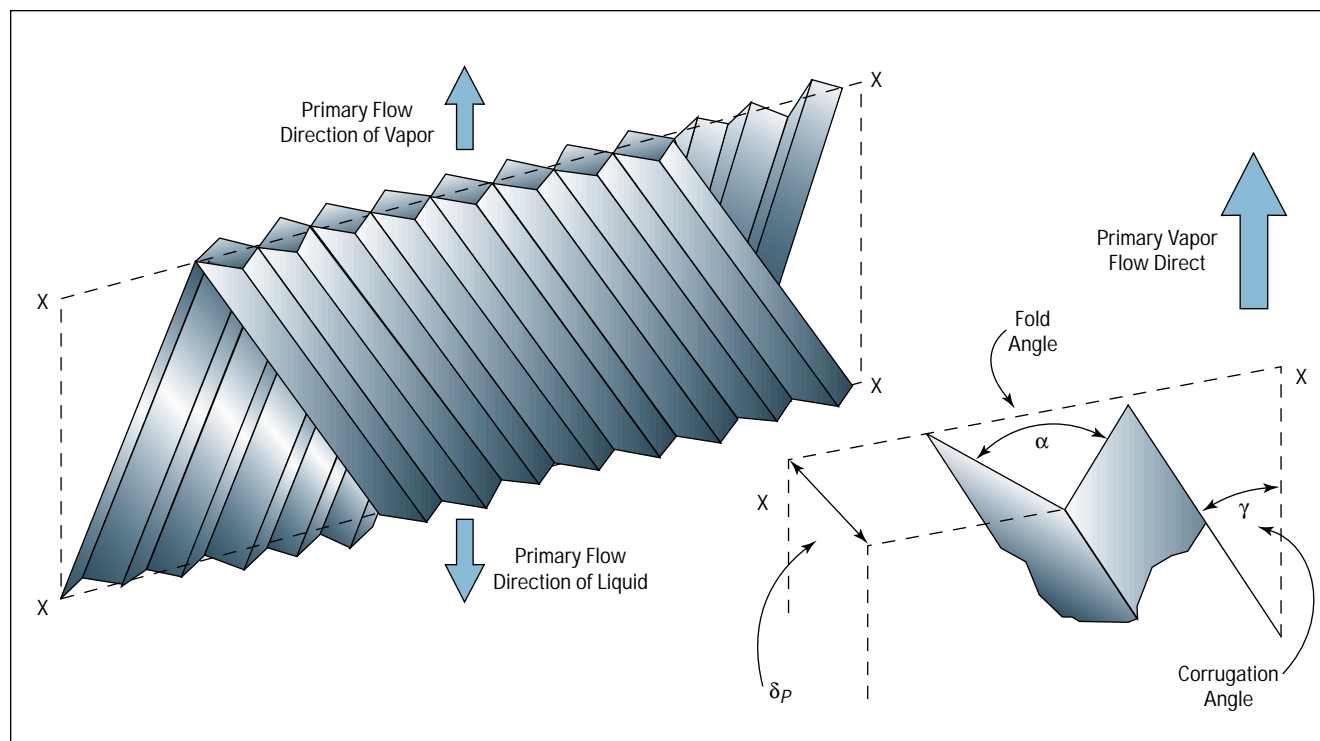
Columns can be divided into two major groups based on the type of packing used — either random (or dumped) packing, or structured (or ordered) packing. Random packings often are either cylindrical (ring) shaped, or half cylinder (saddle) shaped. We will call a single ring or saddle a packing element. Figure 1 il-

lustrates some of the common types of random packing. Both rings and saddles typically have features that are formed into the packing element. These features and other details can provide surface area within the structure, increase resistance to deformation, and also prevent elements from nesting.

Within a packing type, elements are available in a variety of sizes and materials of construction; elements fabricated from a given material look essentially alike except in their size.



■ Figure 1. Types of random-packing elements.



■ Figure 2. Parameters for structured packing.

This means that they are geometricaly similar and differ only by a characteristic dimension, δ_p . We will find this very useful as we develop our theoretical understanding. For random packings, we will define δ_p as the nominal packing size or diameter. As an example, a 25-mm Pall Ring has a nominal diameter and value for δ_p of 25 mm.

Mass transfer occurs at the interface between vapor and the liquid film on the packing surface. The mass transfer is significantly impacted by the specific area of the packing, a_s , and this is controlled by the packing's nominal size. As long as the diameter of the column is very large compared to δ_p , a_s is inversely proportional to δ_p . The constant relating the two depends upon the packing type and how the elements are arranged. For example, if we assume that the packed column is filled with thin-walled cylindrical elements stacked in an ordered fashion with 60° pitch and the elements are just touching, the value for

a_s can be calculated to be about $7.25/\delta_p$. Packing elements installed in a random or dumped fashion orient themselves in an irregular manner, and this impacts the constant relating a_s and δ_p . The constant also can depend upon the ratio of δ_p to the vertical height of the element. In general, for both random rings and saddles, $a_s = 5.7/\delta_p$ within a band of about $\pm 10\%$.

The second general category of packing commonly is referred to now as structured packing. It can be made of woven or solid material, usually metal, which typically is corrugated and bundled into segments that are placed layer by layer into the column shell. Most commercially available structured packings have perforations or texturing through stamping to help promote mixing and liquid spreading, as well as to modestly increase surface area. Figure 2 illustrates the general geometry characteristics of the type of structured packing often used today.

Pressure-drop and mass-transfer

characteristics can be controlled by changing the corrugation angle, γ , the fold angle, α , and the height of the corrugation. We will define the characteristic dimension of structured packing, δ_p , to be the height of the corrugation. Most such packings have a corrugation angle of 45° and a fold angle of 90° ; the height of the corrugation, therefore, is the primary geometry parameter used by the column designer for optimization.

The constant relating a_s to δ_p depends upon α . If we neglect the sheet thickness and any change in surface area resulting from surface texture or perforations, $a_s = (2/\sin(\alpha/2))/\delta_p$. Thus, for the typical fold angle of 90° , $a_s = 2.8/\delta_p$. This shows that the specific area for structured packing is less than that for random packings for a given value of δ_p . Keep in mind, however, that we define δ_p as the corrugation height for structured packing and the nominal packing-element diameter for random packing.

Some mass-transfer fundamentals

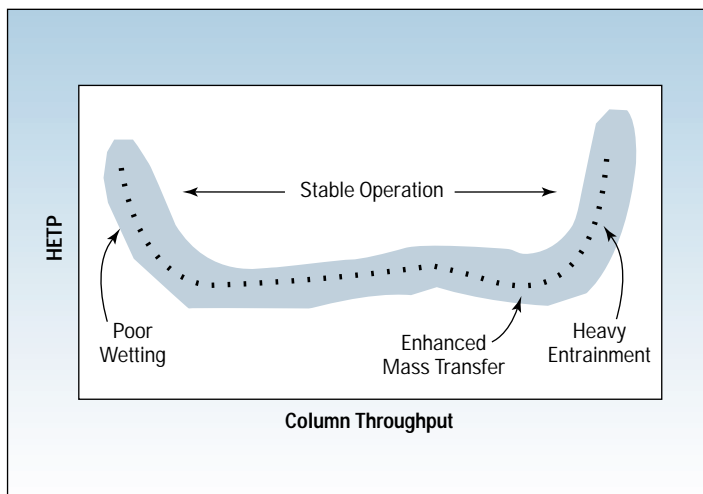
Mass transfer within a packed column typically is described in terms of *HETP*, the height equivalent of a theoretical plate — that is, the height of packing required for a theoretical stage of separation. Figure 3 shows the general relationship between *HETP* and column throughput. Performance remains relatively constant and stable except at both low and high rates. At low liquid rates, sheets of liquid are not stable and rivulets do not spread sufficiently to wet the entire packing surface; so, mass transfer is poor. As column throughput increases, there is a large stable region where packing is well wetted and *HETP* is relatively constant. At the higher-rate portion of the stable region, mass transfer improves (*HETP* gets lower). This improvement is caused by an increase in interfacial area due to liquid waves and entrainment. At higher rates, performance decreases rapidly due to substantial liquid entrainment in the vapor being carried up the column. This entrainment degrades the composition profile and can result in liquid flow and vapor flow redistribution.

Optimization of the packing for (1) maximizing theoretical stages per height of section or column, (2) minimizing pressure drop per theoretical stage of separation, and (3) maximizing the operating range of the column that results in reasonable performance often requires the column to operate at the extremes of the stable operating range. We need, therefore, an understanding of the phenomena that control each of the three regions: poor wetting, stable operation, and heavy entrainment.

Poor wetting

Liquid flows from the distributor onto the packed section as a series of streams. Good wetting, resulting in a substantial fraction of the packing surface area being wet, requires that packing elements or layers of structured packing distribute these

Figure 3. Packing performance.



streams into a combination of rivulets and films that fully migrate throughout the packed column cross-section. The liquid flow rate per wetted perimeter controls liquid-film hydrodynamics. We will designate Γ as the average value for liquid flow rate per wetted perimeter, assuming all of the liquid is uniformly distributed. By mass balance, $\Gamma = L/a_s$, where L is the liquid mass flux flowing down the column. For a given packing type and distillation system, a minimum value for Γ is required for the packing to be substantially wet. We will designate this minimum value as Γ_C ; if Γ is below this value, wetting will be poor, resulting in poor mass transfer and a large *HETP*. Γ_C would be expected to be a function of contact angle and physical properties, and may depend upon packing surface-texture details. It should be a constant, however, for a given distillation system (composition and pressure) and packing type.

Stable operation

Most basic mass-transfer textbooks (for example, Ref. 1) develop equations for continuous distillation assuming a downward flowing liquid phase in contact with an upward flowing vapor phase. A rearrangement of these equations leads to Eq. 1 for the *HETP* vs. the appropriate mass-transfer coefficients (see box below), which can be rearranged to Eq. 2 (see box) where V_s is the superficial velocity of vapor up the column. The term in the bracket is the increase in *HETP* resulting from liquid-phase resistance. Frequently, however, vapor-phase resistance dominates. In such cases, this bracketed term is approximately unity and assuming that k_v can be correlated using the format of Eq. 3 we get: Eq. 4 (see box on next page). Packed column data can be used to arrive at values for p and n , but, by analogy to heat transfer and wetted-wall-column mass transfer, p is ex-

$$HETP = G \left(\frac{1}{\rho_{MV} k_v a_i} + \frac{m}{\rho_{ML} k_L a_i} \right) \frac{\ln \lambda}{\lambda - 1} \quad (1)$$

$$HETP = \frac{1}{a_i} \frac{V_s}{k_v} \left(1 + m \frac{\rho_{MV} k_v}{\rho_{ML} k_L} \right) \frac{\ln \lambda}{\lambda - 1} \quad (2)$$

pected to be about 0.8 and n about 0.3. For the stable region, where packing is assumed to be well wetted, a_i should be inversely proportional to the characteristic dimension of the packing, δ_p . We find, then, that for a given distillation system, *HETP* only weakly depends upon vapor flow (about $V_s^{0.2}$), but strongly depends upon the characteristic dimension of the packing (about $\delta_p^{0.8}$). This weak dependency of *HETP* on V_s is why the concept of *HETP* is so useful.

We also will need a correlation for pressure drop. One based on a significant amount of experimental data is the Eckert Generalized Pressure Drop Correlation for structured packing, this approach defines two axis:

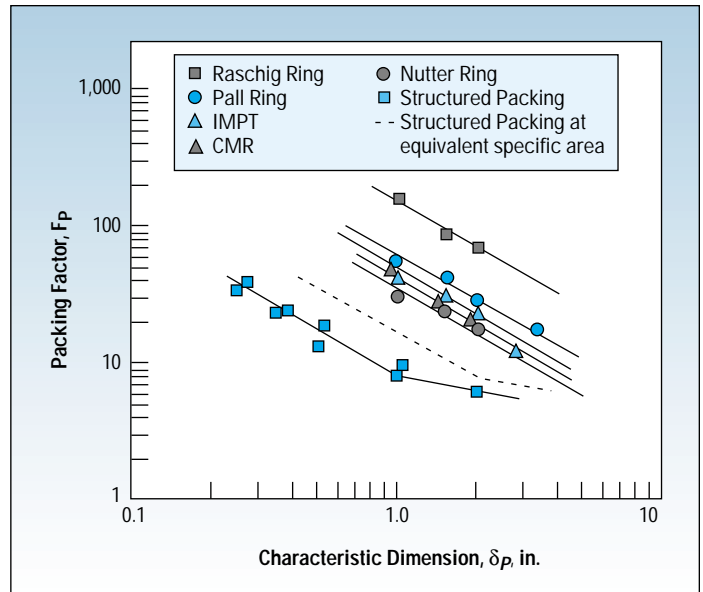
$$Y = V_s \left(\frac{\rho_v}{\rho_L - \rho_v} \right)^{0.5} F_p^{0.5} \left(\frac{\mu_L}{\rho_L} \right)^{0.05} \tag{5}$$

and

$$X = \frac{L}{V} \left(\frac{\rho_v}{\rho_L} \right)^{0.5} \tag{6}$$

This correlation is graphically represented by a plot of Y vs. X along with lines of constant pressure gradient. A key test of the validity of this approach is whether a single value of the packing factor, F_p , adequately agrees with all of the constant-pressure gradient lines. Kister and Gill (2) evaluated structured-packing pressure-drop data and found that a constant value of F_p for structured packing could not be found; they, therefore, redrew the constant-pressure gradient lines for structured packing. The difference in the random-packing and structured-packing constant-pressure gradient lines becomes signifi-

Figure 4. Packing factor dependency on characteristic dimension.



cant for values of X exceeding 0.20, and for values of pressure gradient more than 0.5 in. of water pressure drop/ft of packing height. F_p is purely an experimental constant determined by minimizing the error between the data and the correlation, and is a function of packing type and characteristic dimension.

In Figure 4, we have plotted F_p values from Kister (3) vs. δ_p for several commercial packings. We find that, for a given value of δ_p , F_p for Pall Rings is less than half that of Raschig Rings. This is attributable to the openness of the Pall Rings compared to Raschig Rings. The other random packings show an additional one-third to one-half reduction in F_p , resulting from further increases in perforations of the element and, for some elements, a reduction in element height that allows elements to

stack in a more open manner. For structured packing, for equal values of δ_p , F_p is about one-fourth of the minimum value for random packing. But, because the definition of δ_p for random and structured packing differ, a comparison of values of F_p at equivalent specific area is more appropriate. We find that structured packing values for F_p are about one-half the lowest value for random packings at equal specific area.

For low and moderate loading, pressure drop is directly proportional to the value for F_p ; therefore, the pressure drop for structured packing is about one-half that of the lowest-pressure-drop random packings at equivalent values of specific area and equal column throughput.

With reasonable accuracy, a curve-fit of published values for F_p is:

$$F_p = C_3 (\delta_p)^{-1.1} \quad \text{with } \delta_p \text{ in inches} \tag{7}$$

Alternatively, because a_s is inversely proportional to δ_p ,

$$F_p = C_4 (a_s)^{1.1} \quad \text{with } a_s \text{ in ft}^2/\text{ft}^3 \tag{8}$$

The values of C_3 and C_4 are given in Table 1 and are important when we look at optimization for different types of packings.

The Eckert-type correlation does not allow easy identification of the

$$\frac{k_v \delta_p}{D_v} = C_1 \left(\frac{\rho_v V_s \delta_p}{\mu_v} \right)^p \left(\frac{\mu_v}{\rho_v D_v} \right)^n \tag{3}$$

$$HETP = \frac{C_2}{a_i} \left(\frac{V_s \delta_p}{D_v} \right)^{1-p} \left(\frac{\mu_v}{\rho_v D_v} \right)^{p-n} \frac{\ln \lambda}{\lambda - 1} \tag{4}$$

functionality that relates pressure drop to flow and geometry parameters. An explicit correlation would be helpful for our optimization effort. Liquid, as it flows down the packed column, raises pressure drop by: (1) increasing the roughness, (2) taking up space, which, in turn, boosts vapor velocity at a given mass throughput, and (3) providing liquid droplets that become entrained in the vapor core. Because the first mechanism dominates except near flood, we will use a correlation format similar to that used to calculate pressure drop for fully turbulent vapor flow in rough tubes:

$$\frac{\Delta P}{\Delta Z} = A \left(\frac{\epsilon_p}{\delta_p} \right)^B \frac{\rho_v}{\rho_L} \frac{V_S^2}{g \delta_p} \quad (9)$$

The pressure gradient $\Delta P/\Delta Z$ is expressed in units of height of liquid per height of packing, ϵ_p is the height of liquid-flow-induced roughness, and g is acceleration due to gravity, which is required as we are expressing pressure drop in terms of liquid height. A and B are constants that we will borrow from rough tube data. We will assume that ϵ_p can be approximated from the average height of the liquid film; this can be calculated from a simple force balance, yielding:

$$\delta_F = \left[\frac{3 \mu_L \Gamma}{\rho_L (\rho_L - \rho_v) g} \right]^{0.33} \quad (10)$$

where Γ is the average mass-flow rate of liquid per wetted surface. From before, we know that $\Gamma = L/a_s$, and, because a_s and δ_p are inversely proportional, $\Gamma \propto L \delta_p$. Substitution gives: Eq. 11 (see box below). Based on rough-tube pressure-drop data, B is about 0.25. The constant A_1 is expected to vary for different types of

$$\frac{\Delta P}{\Delta Z} = A_1 \left[\frac{3 \mu_L L}{\delta_p^2 \rho_L (\rho_L - \rho_v) g} \right]^{0.33B} \frac{\rho_v}{\rho_L} \frac{V_S^2}{g \delta_p} \quad (11)$$

Table 1. Constants for Eqs. 15 and 16.

Type of packing	C_3	C_4
Raschig Rings	140	1.35*
Metal Pall Rings	62	0.66
Intalox Metal Tower Packing	39	0.37*
Cascade MiniRings	42	0.34
Nutter Rings	35	0.34*
Hiflow Rings	34	0.33
Structured Packing ($\alpha = 90^\circ, \gamma = 45^\circ$)	8	0.137

Note: published values used for a_s when available; when unavailable (indicated by an asterisk), the approximate relationship, $a_s = 5.7/\delta_p$, was used.

packing elements but, for geometrically similar packings, should be constant for elements fabricated from the same type of material. The variation in A_1 values for different types of packing is identical to the variation in the constants C_3 and C_4 that relate the packing factor to δ_p and a_s . Manufacturing techniques for metal, plastic, and ceramic materials differ, however, resulting in some differences in element geometry even if elements are part of the same packing type. Thus, A_1 will vary depending upon material of fabrication. This expression for the pressure gradient is not a complete representation of pressure drop, but still has significant similarities with the Eckert-type pressure-drop correlation, especially in the nonloaded region (specifically at values of X less than 0.5, where pressure drop is largely a function of Y^2). We expect that, for this non-heavily-loaded region, there is a weak dependency on liquid mass flux (about $L^{0.08}$). Also, for geometrically similar packings, F_p is approximately inversely proportional to the characteristic dimension (about $\delta_p^{-1.15}$). These trends will be useful as we draw conclusions about the optimization of packed columns.

Heavy entrainment

We also will need an understanding of packed column flooding. As column throughput increases beyond the stable operating region, pressure drop begins to rise much more quickly, due to more liquid entrainment in vapor and a greater vapor velocity resulting from higher liquid holdup. In addition, mass transfer begins to drop as increased liquid entrainment flows up the column. At very high throughput rates, substantial quantities of liquid flow up portions of the column. Because packing is relatively open to cross-flow, liquid and vapor tend to redistribute themselves; so, local values of L/V vary substantially, resulting in a sharp dropoff in column mass transfer. In packed columns, there is no discrete flood point, but operation of a column anywhere within this very heavily loaded region is undesirable. A force balance between the upward pressure drop force on a liquid film and the downward gravity force gives at flood:

$$\delta_p \left. \frac{\Delta P}{\Delta Z} \right|_{Flood} = A_2 \delta_F \quad (12)$$

If we define f_{LFlood} to be the liquid void fraction at flood, then $f_{LFlood} = a_s \delta_F$. Because a_s is inversely proportional to δ_p , we have the interesting relationship:

$$\left. \frac{\Delta P}{\Delta Z} \right|_{Flood} \propto f_{LFlood} \quad (13)$$

for any particular packing type.

This force balance, coupled with the equation for δ_F , and our understanding that Γ is proportional to L

δ_p , predicts that the pressure drop resulting in flooding is proportional to $\delta_p^{-0.8}$. It also indicates that film thickness plays some role. In support of this force-balance approach, we can use the empirical Kister and Gill correlation for packing flooding (4), Eq. 14 in box below. This correlation does not agree with the dependency on liquid rate (the dependency on δ_p) predicted by the force balance, but, because we have shown that F_p is proportional to $\delta_p^{-1.1}$, the Kister and Gill correlation for flooding does indicate that the pressure-drop gradient at flood is proportional to $\delta_p^{-0.77}$, which is identical to our force-balance-approach prediction.

The approach used

We now can combine these equations derived from mass-transfer and pressure-drop fundamentals and look at their implication on column optimization. Due to decreasing cost and several performance advantages, structured packing is becoming more popular. We, therefore, will address column optimization for structured packings and then discuss, for each optimization goal, the approach for random packings.

To minimize *HETP*:

We will assume that gas-phase resistance dominates and packing is fully wet such that a_i is proportional

to $\delta_p^{-1.0}$. We also will assume that the values for p and n are 0.8 and 0.3, respectively. Therefore, we get Eq. 15 (see box below).

Most vendors of structured packing have standardized on corrugation angle and fold angle, namely, $\gamma = 45^\circ$ and $\alpha = 90^\circ$; therefore, in general, metal structured packings from different vendors are very similar with the possible exception of surface details. These surface differences can have some impact on the liquid resistance, but we are assuming for this analysis that vapor-phase resistance dominates. For structured packing when $\alpha = 90^\circ$ and $\gamma = 45^\circ$, this equation for *HETP* shows that, for a given separation system and column throughput, the only geometry variable that significantly impacts *HETP* is δ_p . Smaller values of δ_p give greater values of specific area, a_s , and lower section heights or more mass transfer within a given section height. This equation predicts that *HETP* depends upon $\delta_p^{1.2}$ (or $a_s^{-1.2}$), which is very close to the results from published data.

To minimize pressure drop per theoretical stage of separation:

We observe the relationship given in Eq. 16 (see box below) from the equations for pressure drop and *HETP*.

As discussed before, within a

packing family, for example, Pall Rings or structured packing with uniform corrugation and fold angles, A_1 and C_5 are constant. Therefore, within a packing family and for a given distillation system:

$$\frac{\Delta P}{\Delta Z} \frac{L}{HETP} \propto a_s^{2.35} V_s^{1.8} L^{0.08} \quad (17)$$

Reducing the vapor throughput will decrease pressure drop, but will substantially increase capital investment and is rarely justifiable. Selecting a lower value of a_s to give sufficient *HETP*, but at an acceptable pressure drop, is the typical optimization.

To maximize the stable operating range:

For packed columns, the range of stable *HETP* performance is bounded at high throughputs by high pressure drop and poor mass-transfer performance as flooding is approached, and at low throughputs by poor performance resulting from inadequate wetting. The characteristic dimension impacts packed column flooding in two ways. First, pressure drop for a given vapor throughput is approximately inversely proportional to δ_p . Second, as δ_p gets smaller, the pressure drop that will result in flood is approximately inversely proportional to δ_p . The net result is that for geometrically similar packing:

$$K_{V\text{Flood}} \propto \delta_p \quad (18)$$

For a given distillation system and design L/V , there is a minimum Γ_C . We can show that:

$$K_{V\text{Min}} \propto \delta_p^{-1.0} \quad (19)$$

Maximizing the range for stable operation is equal to maximizing $K_{V\text{Flood}}/K_{V\text{Min}}$, which depends upon δ_p^2 . Larger values of δ_p will result in a significantly larger operating range at the expense of reduced mass-transfer performance.

For high turn-down service, distributor design poses a further complication. Close work with the vendor, along with thorough full-scale testing, at least with water, often is important (5,6).

$$\left. \frac{\Delta P}{\Delta Z} \right]_{\text{Flood}} = 0.115 F_p^{0.7} \quad \text{with } F_p \text{ in inches of water} \quad (14)$$

$$HETP = C_5 \delta_p \left(\frac{V_s \delta_p}{D_v} \right)^{0.2} \left(\frac{\mu_v}{\rho_v D_v} \right)^{0.5} \frac{\ln \lambda}{\lambda - 1} \quad (15)$$

$$\frac{\Delta P}{\Delta Z} \frac{L}{HETP} = A_1 \left[\frac{3 \mu_L L}{\delta_p^2 \rho_L (\rho_L - \rho_v) g} \right]^{0.083} \frac{\rho_v}{\rho_L} \frac{V_s^2}{g \delta_p} / C_5 \delta_p \left(\frac{V_s \delta_p}{D_v} \right)^{0.2} \left(\frac{\mu_v}{\rho_v D_v} \right)^{0.5} \frac{\ln \lambda}{\lambda - 1} \quad (16)$$

Summary of optimization rules

To maximize the number of theoretical stages for a given section height:

For structured packing:

1. Use packing with a high specific area, and run the column near the upper range of stable operation. Be careful of packings with very high specific areas, especially for low-pressure distillation when low liquid throughputs are common and partial wetting may occur — this reduces the advantage of using a higher specific area to decrease *HETP*. Recognize that operating range will be decreased significantly as specific area increases.

2. Use packings with a corrugation angle of 45°.

3. Be concerned about the need for redistribution, which is related more to theoretical tray count in a section than section height.

For other types of packing:

Use random packing elements with small values of δ_p , and run the column near the upper range of stable operation. When looking at different types of random packing, those that have larger specific areas for a given characteristic dimension will tend to have better values of *HETP*. In addition, because pressure drop generally enhances mass transfer, consider packing types with somewhat higher pressure drop (for example, higher values of C_3 and C_4) — but this can decrease capacity and require a larger diameter column. The cost of high-specific-area random packings often is much higher than that of structured packing — therefore, when maximizing the number of theoretical stages within a given section height, it is hard to beat structured packing.

To minimize the pressure drop per theoretical stage:

For structured packing:

We wish to minimize $a_s^{2.35} V_s^{1.8} L^{0.08}$.

1. Reducing the vapor velocity will decrease pressure drop per theoretical stage, but will increase column diameter — the additional capital investment rarely is justified.

2. Decreasing the specific area a_s will reduce pressure drop per theoretical stage. If an equal number of stages are required, column height will increase.

3. Using structured packing with a 30° corrugation angle can give a modest improvement in pressure drop per theoretical stage, but also will result in a higher *HETP*. This usually is not cost-justified; increasing the characteristic dimension while keeping a 45° corrugation angle often is a better solution.

For other types of packing:

Rules 1 and 2 also apply to random packings. There are many types of random packing, and this results in a relatively wide range of pressure drop for a given characteristic dimension. This is shown by the range in values for constants C_3 and C_4 . The total pressure drop stems from bluff-body losses and shear-stress losses at the surface. Bluff-body losses generate turbulence in the main vapor core, while shear-stress losses result in turbulence at the packing surface. Because most of the mass transfer in a packed column occurs near the packing surface, packings with lower bluff-body losses usually give better mass-transfer performance for a given pressure drop. Such packings result in significant contact area, but generally are more open or preferentially lie in a manner that results in a more open pattern. These packings have lower pressure drop for a given specific area or characteristic dimension. This means that packings with lower values of constants C_3 and C_4 are preferred. Structured packing, however, has a significantly lower pressure drop for a given specific area than random packings — therefore, structured packing usually is preferred when minimizing pressure drop per theoretical stage.

To maximize the operating range:

For structured packing:

1. The primary variable that impacts operating range is the characteristic dimension or the packing specific

area. Larger values of δ_p will increase operating range, but will result in a higher *HETP* and a taller column for a given number of theoretical stages.

2. Some increase in range is possible by changing the corrugation angle to yield less pressure drop for a given vapor throughput — for example, using a 30° corrugation angle instead of the more typical 45°. This change, because it reduces pressure drop, will increase capacity without significantly changing Γ_C . Because Γ_C has not changed, the drop-off in performance at low rates due to poor wetting still will be the same and operating range is enhanced. Structured packing with a 30° corrugation angle, however, will have a higher *HETP* and less vapor mixing — that may be a concern for column sections requiring a large number of theoretical stages.

3. Full wetting is promoted by capillary forces; so, packings made of woven materials are particularly attractive when the column is operating with very low liquid rates. This is particularly true for high-vacuum distillations or when poor wetting fluids such as water are distilled or when a very large operating range is required.

4. The operating range of internals, especially liquid distributors and redistributors, often can be the controlling factor. The requirement for uniformity of the local L/V is particularly important for column sections with significant theoretical-stage count.

For other types of packing:

As with structured packings, increasing δ_p increases the maximum operating range for random packings, but at the expense of intrinsically poorer *HETP*. Packings that have lower pressure drop for a given value of δ_p also will have inherently higher operating range — such packings are those with lower values for constants C_3 and C_4 . Finally, packing elements with surface texturing or materials that tend to better wet with the system will enhance the maximum allowable operating range.

Trays vs. packing

Clearly, both trayed and packed columns will continue to have significant roles to play in distillation. Understanding the factors involved in optimizing each provides a basis for choosing between trays and packing. Here are some general guidelines:

1. When the service is nonfouling, either type of column can be designed to yield comparable theoretical stage counts per section height. Packing has the disadvantage of requiring redistributors if large stage counts within a column section are required.

2. Fouling can pose problems for both trays and packing.

3. Packed columns often can be designed with greater stable operating range than sieve trays. Valve and bubble-cap trays can have a stable operating range equal to or even greater than that of columns with random or normal corrugated structured packing. Structured packing made of expensive woven materials can have a very broad operating range. The design of internals for a stable operating range of more than two or three is much more difficult for packings than for trays.

4. For applications requiring low pressure drop per theoretical stage, packing has a significant inherent advantage, because the interfacial area for packed columns is generated through liquid spreading on the packing surface — this is a low-pressure-drop phenomenon compared to the mechanism required to generate high mass-transfer efficiency within a trayed column.

5. For low-pressure distillation applications, liquid flow rates tend to be very low. The resulting modest liquid inventory fosters spray-like conditions with trays that, in turn,

promote high entrainment and low tray efficiency. This can be mitigated with small perforations, but an alternative is to opt for packed columns if liquid rates are sufficient to obtain good wetting. An added advantage for packing is its inherently lower pressure drop, which is particularly important for low-pressure applications.

6. Tray columns are intrinsically lower cost than packed columns, because far less surface is needed for trays than for packings, and trays require far-lower-cost internals than packings. CEP

Nomenclature

a_i	= interfacial area per packing volume
a_s	= surface area of packing/volume of packing
A	= unspecified constant
A_1	= unspecified constant
A_2	= unspecified constant
B	= constant estimated at 0.25
C_1	= unspecified constant
C_2	= unspecified constant
C_3	= constant relating F_p to δ_p , expressed in inches
C_4	= constant relating F_p to a_s , expressed in ft ² /ft ³
C_5	= unspecified constant
D	= molecular diffusivity
f_{LFlood}	= liquid void fraction at flood
F_p	= packing factor
g	= acceleration due to gravity
G	= vapor molar flux
$HETP$	= height equivalent to a theoretical plate
k_L	= liquid-phase mass-transfer coefficient
k_V	= vapor-phase mass-transfer coefficient
K_V	= density-corrected superficial velocity within column, $[\rho_V/(\rho_L - \rho_V)]^{0.5} V_S$
L	= liquid mass-flow rate through column
m	= slope of equilibrium curve
$\Delta P/\Delta Z$	= packed-column pressure-drop gradient, expressed in height of liquid/height of packing
p	= constant estimated at 0.8
n	= constant estimated at 0.3
V	= vapor mass-flow rate through column
V_S	= superficial velocity of vapor
X	= x-axis on Eckert Generalized Pressure Drop Correlation
Y	= y-axis on Eckert Generalized Pressure Drop Correlation

Greek letters

α	= structured-packing fold angle, see Figure 2
γ	= structured-packing corrugation angle, see Figure 2
δ_F	= liquid film thickness
δ_p	= characteristic dimension: for random packing, nominal packing size; for structured packing, corrugation height
ϵ_p	= roughness attributable to liquid waves
Γ	= average mass-flow rate of liquid per wetted surface
Γ_C	= minimum mass-flow rate per wetted surface
λ	= ratio of slope of equilibrium line, m , to operating line, L/V
μ	= molecular viscosity
ρ	= density

Subscripts

L	= liquid
V	= vapor
ML	= liquid molar
MV	= vapor molar
$Flood$	= at flood
Min	= minimum column throughput for region of stable operation

Literature Cited

1. **Treybal, R. E.**, "Mass Transfer Operations," McGraw-Hill, New York, p. 250 (1968).
2. **Kister, H. Z., and D. R. Gill**, "Distillation and Adsorption," presented at IChemE meeting, Birmingham, U.K. (Sept. 1992).
3. **Kister, H. Z.**, "Distillation Design," McGraw-Hill, New York, p. 495 (1992).
4. **Kister, H. Z., and D. R. Gill**, "Predict Flood Point and Pressure Drop for Modern Random Packings," *Chem. Eng. Progress*, **87** (2), p. 32 (Feb. 1991).
5. **Olsson, F. R.**, "Detect Distributor Defects Before They Cripple Columns," *Chem. Eng. Progress*, **95** (10), p. 57 (Oct. 1999).
6. **Bennett, D. L., and K. A. Ludwig**, "Understand the Limitations of Air/Water Testing of Distillation Equipment," *Chem. Eng. Progress*, **90** (4), p. 72 (Apr. 1994).

D. L. BENNETT is General Manager, Advanced Gas Separation, for Air Products and Chemicals, Inc., Allentown, PA ((610) 481-7788; Fax: (610) 706-7420; E-mail: bennetd@apci.com). For more background on the author, see p. 26.